

Applying Bidirectional Crossbar Switches with Extra Sets of Inlets and Outlets to Three-Stage Clos Networks

Labson¹ and Hitoshi Obara^{2*}

^{1,2*}Graduate School of Engineering Science, Akita University, Japan
¹labinct@gmail.com, ^{2*}obara@ee.akita-u.ac.jp

Abstract

In scaling up optical network capacity in space-division multiplexing, the three stage Clos network has been used for building high port count switches with reduced Crosspoint. This paper presents a new three stage Clos architecture with extra internal routes yielding a smaller number of crossbar switches. The three-stage Clos network, denoted by $C(n, m, r)$, where n , m , and r represent the number of input (output) ports of the input (output) switches, the number of middle switches, and the number of input and output switches, respectively, is widely used. Here, we consider Clos networks that include conventional crossbar switch elements, which are composed of 2×2 basic cells often used in optical networks. First, we point out that the crossbar switches have a number of idle ports unused, and discuss how they can be employed to improve the network performance. We then introduce a new type of Clos network in which the middle stage is composed of bidirectional crossbar switches with extra sets of inlets and outlets. This is done by utilizing the idle ports on the crossbar switches. Second, we elaborate on the non-blocking performance of this network and show that the theoretical lower bound of m for rearrangeable non-blocking capability can be reduced by 25% of the original Clos network when idle ports are used. We also demonstrate that when $m = n$, the number of rearrangements is reduced to one at most, regardless of the values of n and r , while typical Clos networks require $r - 1$ rearrangement in worst-case scenarios. Finally, we show that m in the wide-sense non-blocking bidirectional Clos network can be approximately 25% lower than in the conventional strictly non-blocking Clos network. With this result, the architecture can be applicable to three stage clos networks where the size of the middle switches is larger than that of inputs and outputs stages.

Keywords: Switch network, Three-stage clos network, Non-blocking condition, Bidirectional switches, Rearrangeable non-blocking switch, Wide-sense non-blocking switch

1. Introduction

Since C. Clos published his seminal work on three-stage switch networks, the Clos architecture has been the most practical and Crosspoint-efficient design principle for large switching networks [1]. In fact, in many previous studies, the Clos architecture was applied to various types of switches, including space-division multiplexed switches [2], time-division multiplexed switches [3], packet switches [4], and optical switches [5]. In this study, we considered a space-division multiplexed Three-Stage Clos Network (TSCN) with non-blocking capability for unicast connection requirements. We assumed that every stage consists of

Article history:

Received (January 27, 2021), Review Result (March 18, 2021), Accepted (June 19, 2021)

conventional crossbar switches (XBSs), which are composed of 2×2 basic switch elements (BSEs) arranged in a square array [6].

Recently, a modified type of XBS in which the idle ports are used as an extra set of inputs and outputs attracted the interest of researchers. For example, a single-stage architecture using the modified XBS was shown to decrease the number of Crosspoint while maintaining the simplicity of the routing control [7][8]. Cascaded and parallel two-stage switches leveraging the modified XBSs were also investigated as a method for scaling switch sizes [9][10]. However, prior studies focused only on single- and two-stage switch configurations. Conventional TSCNs have internal routes fewer than can be provided if idle ports in their XBSs were utilized. We expect that when the modified XBSs are used in TSCNs, the extra ports will provide additional internal routes without increasing the size of XBSs. This will eventually yield a smaller number of XBSs, Crosspoint, and/or rearrangements. In this study, we discuss through theoretical analysis how the modified XBS can be applied to TSCNs and describe how the switch performance in terms of non-blocking properties and Crosspoint scalability of TSCNs can be improved with the introduction of additional routes.

The rest of the paper is organized as follows; In section 2, we refer to related works and give the approach of our work. In Section 3, we briefly outline TSCNs and modified XBSs and introduce some particular definitions and notations for this study. In Section 4, we present a new design for TSCNs in which the modified XBSs are used in bidirectional mode. In Section 5, we elaborate on the theoretical lower bound of the number of middle switches for bidirectional TSCNs. We also identify the maximum number of rearrangements in the typical case $m = n$. In Section 6, we suggest a new Wide-Sense Non-Blocking (WSNB) condition for bidirectional TSCNs. Section 7 gives the methodology of our study and verifies the WSNB properties of the proposed switch through computer simulations. Section 8 presents the results of the simulations. We discuss switch performance trade-offs in bidirectional TSCNs. We also discuss the implications of our results. Finally, the paper concludes in Section 9.

2. Related works

Clos networks were at the beginning invented for application in telephone exchange systems. However, recently it has been used in wide-ranging applications such as electrical and optical cross connects which are essential for building communication networks that are economical with highly multiplexed signal links [11]. Clos networks have been classified based on their connecting capabilities. Some have been classified as Strictly Non-Blocking (SNB) network [12], Rearrangeably Non-Blocking (RNB) [13], wide sense non-blocking [14] and repackable networks [15]. In [16], a component efficient design for a parallel optical XBS which utilizes the idle ports as extra input ports and/or output ports was proposed. It was observed that conventional parallel XBSs composed of 2×2 BSE have a significant number of idle internal routes between its idle ports. The author also reported a switch with reduced Crosspoint count from N^2 to $3N^2/4$, where N is the switch size. This was only applied in a single and two stage architectures. Here we focus on applying it to the three-stage switch architecture. Single stage crossbar switch architectures do not fit for dilation as their Crosspoint size increase proportionally to N^2 . Multistage has been the solution to this problem. In [17][18], a Clos unidirectional network-on-chip (Clos-UDN) packet switch was proposed which focused on traffic balancing and congestion management. The whole XBS was replaced by a crossbar-like Network-on-Chip (NoC) operating in unidirectional mode. The study proposed a use of multi-hop NoC as a crossbar with inter router wires that were shorter compared to those in a single-hop conventional crossbar. Hassen and Mhamdi et al. [19][20] proposed a three-stage Clos

network switch based on multi-directional NoCs (MDN central modules). Both of these works involved replacing the conventional crossbars by UDN and MDN modules respectively. MDN modules are modified version of UDNs switches with inputs/outputs ports operating in multidirectional mode. The NoC based crossbar modules are expensive because increasing the port count involves large NoC modules which ultimately increases the cost of designing them. Multi-hop interconnects have a higher latency than the single-hop in the conventional crossbar.

Also, larger NoC modules are needed to perform well under critical traffic. The focus of the above works was on congestion avoidance and load balancing while the focus of our research is modifying the conventional XBSs and analyzing how the TSCN non-blocking properties varies with respect to the number of middle stage switch requirements and scalability of Crosspoint count. We focus on a space switch. The scheduling algorithm and the study of arrival traffic patterns in these switches is beyond the scope of this study.

In this study, for the first time to the best of our knowledge, we stress the potential capabilities of bidirectional TSCNs from the viewpoint of switch structure. Discussions about the types of XBSs potentially suitable for bidirectional switches and how signal performance is affected in bidirectional XBSs are also beyond the scope of this study. However, we believe that conventional optical switches implemented with optical fibers and optical waveguide devices [21] can be used as bidirectional switches. For example, the validity of bidirectional port assignment in an optical XBS was experimentally verified [22].

3. Outline of TSCs and modified XBSs

A typical TSCN, denoted by $C(n, m, r)$, is shown in [Figure 1], where n , m , and r represent the number of input (output) ports of input (output) switches, the number of middle switches, and the number of input and output switches, respectively. The switch size of the TSCN is represented by $N \times N$, where the first and second terms are the number of input and output ports, respectively, and $N = nr$ holds. We assume that every XBS in [Figure 1] consists of 2×2 BSEs arranged in a square array often used in optical switches, as shown in [Figure 2a]. Here, each BSE has two connection modes, namely cross and bar [Figure 2b] and [Figure 2c], respectively, and is initially set to the cross state. When a connection request between i_j and o_k is issued in an XBS, the BSE at the intersection of the j -th row and the k -th column is flipped to the bar state, and the connection is provided over a rectangular route. We also assume non-blocking TSCNs, i.e., TSCs in which $m \geq n$. The non-blocking capability of conventional TSCs depends on m ; when $m = n$, the TSCN is Rearrangeably Non-Blocking (RNB) and requires rearrangement of $r - 1$ existing calls for setting up a new call in a worst-case scenario. When $m = \lfloor 2n - n/F_{2r-1} \rfloor$, where $\lfloor * \rfloor$ denotes a floor function and F_k is the k -th Fibonacci number, the TSCN is WSNB [23]. No rearrangements are then required, but a complex routing algorithm is necessary. When $m \geq 2n - 1$, the TSCN is Strictly Non-Blocking (SNB) and does not require any rearrangements or designated routing algorithms. For the WSNB TSCN, m approaches $2n - 1$ when $n = r$ and $n \rightarrow \infty$. The non-blocking capabilities in the range $m = n + 1$ to $2n - 2$ are still incompletely understood [24]. Hereafter, we will use four terms, namely ‘input,’ ‘inlet’, ‘output’, and ‘outlet’, in specific ways. The terms ‘input’ and ‘output’ will refer to the TSCN’s ports through which external signals can enter and exit, respectively, while the terms ‘inlet’ and ‘outlet’ will refer to the ports of each XBS dedicated to interconnection between XBSs.

Note in [Figure 2a] that there are idle ports on the top and right sides of XBSs that are reserved for scaling. When the XBS sizes are fixed, it is natural to use them as additional inlets and outlets for interconnection within a single XBS for single-stage configurations [7] or between two XBSs for two-stage configurations [9]. Two types of modified XBS, with unidirectional and

bidirectional modes respectively, were suggested in [10]. These are shown in Fig. 3, where inlets (outlets) are numbered in ascending order from top (left) to bottom (right), i.e., 1 to p (q), respectively. Note that extra sets of inlets and outlets are identified by a prime mark, as in i'_j and o'_k , and their locations differ between [Figure 3a] and [Figure 3b]. Note also that the bidirectional modified XBS has a symmetric port assignment, i.e., each row (column) accepts (emits) a pair of signals from both ends. The unidirectional type, in contrast, is asymmetric; for example, the number of inlets on the left side is different from that on the top. In a preliminary study of ours [10], we observed that the application of bidirectional XBSs to TSCNs is relatively easy owing to their symmetry. Thus, we focused on bidirectional XBSs in this study. Note that the bidirectional modified XBS with p rows and q columns shown in [Figure 3b] has $2p$ inlets and $2q$ outlets. However, we refer to it as the $p \times q$ bidirectional XBS because it cannot accept up to $2p$ input and $2q$ output signals, as described later.

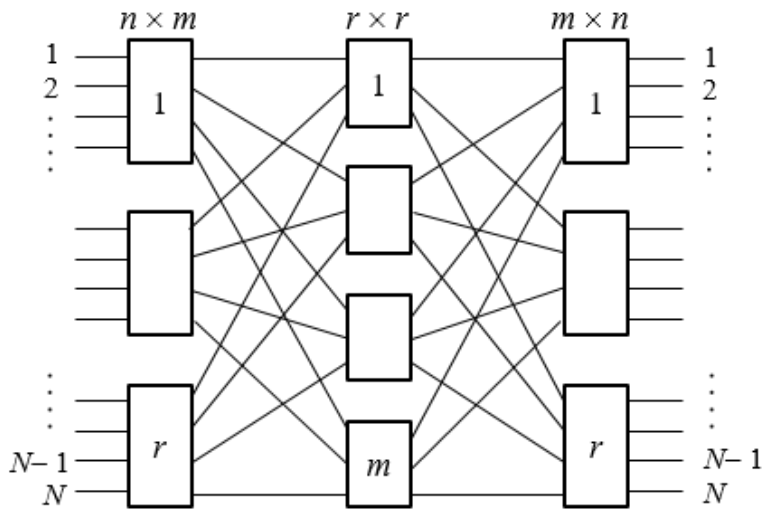


Figure 1. $N \times N$ three-stage Clos network, denoted by $C(n, m, r)$, under consideration in this study. Each stage is composed of $n \times m$, $r \times r$, or $2m \times n$ XBSs

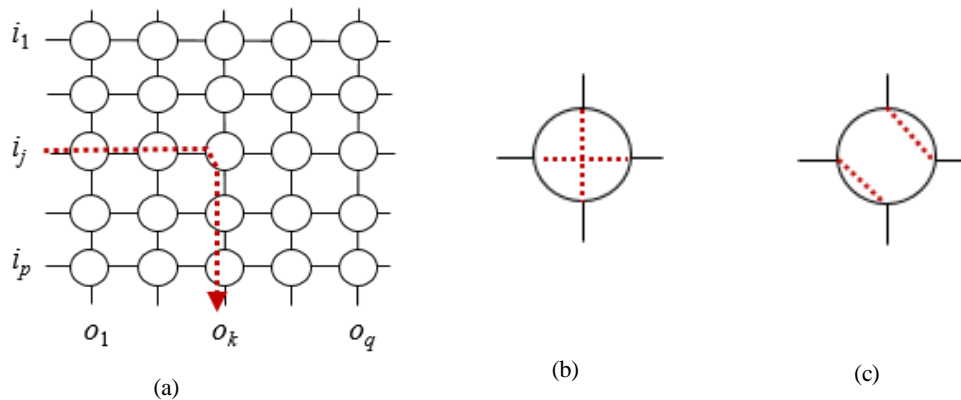


Figure 2. Crossbar switch composed of 2×2 BSEs. (a) Square-array configuration and rectangular route between i_j and o_k ; (b) Default cross state of a BSE; (c) Bar state of a BSE

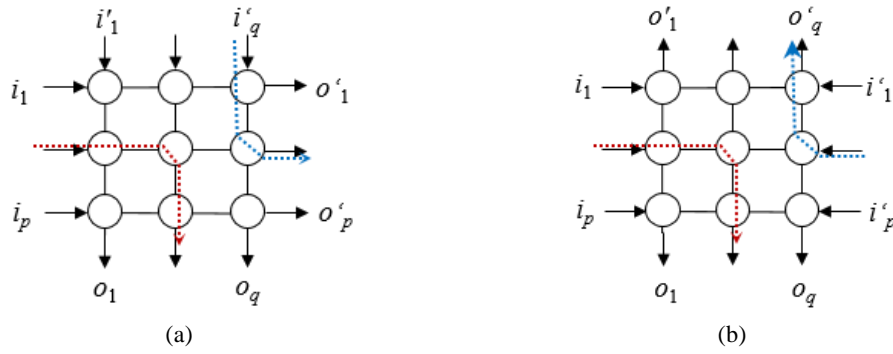


Figure 3. Two possible types of modified XBSs. (a) Unidirectional modified XBSs restrict signals to flow in one direction in each row and column; (b) Bidirectional modified XBSs have a symmetric input/output port assignment and allow signals to flow in two directions in a disjoint manner

4. General description of bidirectional TSCs

Let us begin with a generalized structure of a bidirectional TSCN, denoted by $C_B(n, m, r)$ and shown in Fig. 4. For the sake of simplicity, only a portion of the switch links between stages are depicted. Similar to conventional TSCNs, the $C_B(n, m, r)$ consists of three stages. Each stage is composed of identical XBSs indexed as I_x , M_y , or O_z ($1 \leq x \leq r$, $1 \leq y \leq m$, $1 \leq z \leq r$). In the middle stage, conventional $r \times r$ XBSs serve as $r \times r$ bidirectional XBSs with extra sets of r inlets and r outlets. Note that a pair of links is provided between I_x (O_z) and a row (column) of M_y , respectively, while only a single link is provided there in conventional TSCNs. As a result, M_y may accept (emit) up to two input (output) signals between I_x (O_z) and M_y , respectively. For example, when one inlet i_j ($1 \leq j \leq r$) corresponds to an outlet o_k ($1 \leq k \leq r$), the other inlet i'_j may correspond to o'_l ($1 \leq l \leq r$ and $l \geq k$). This is shown in [Figure 5a] two signals may simultaneously coexist in a single column in a disjoint manner. Similarly, when one input signal from i_j is routed to o_k , the other outlet o'_k may accept another input signal from i'_h ($1 \leq h \leq r$ and $h \leq j$). This is shown in [Figure 5b] two signals may simultaneously coexist in a single row. The sharing of columns and rows may reduce the number of middle switches; however, it can also cause blocking. We discuss how to resolve or avoid blocking in Sections 5 and 6.

The input switch I_x ($1 \leq x \leq r$) is an $n \times 2m$ ordinary XBS in which o_{2y-1} and o_{2y} ($1 \leq y \leq m$) are connected to i_x and i'_x of the middle switch M_y . Note that both i_x and i'_x of M_y may have an input signal, as shown in Fig. 5a. This duplication, on the one hand, can improve the routing performance of the bidirectional TSCN. On the other hand, however, the number of outlets of I_x becomes twice as large as that of a conventional input switch, resulting in an increase in crosspoints. Similarly, the output switch O_z is an ordinary $2m \times n$ XBS. Note that o_k and o'_k of M_y , with $1 \leq k \leq r$ and $1 \leq y \leq m$, are connected to i_{2y-1} and i_{2y} of O_k . Both i_{2y-1} and i_{2y} of O_k may simultaneously receive signals from o_k and o'_k in M_y , as shown in Fig. 5b. As a result, the total number of crosspoints in the input and output switches of the bidirectional TSCN becomes twice as large as that of a conventional TSCN. Nevertheless, if the total number of crosspoints in the middle switches can be reduced by more than the increase in crosspoints in the input and output switches, excellent performance can be achieved at the cost of an increase in crosspoints, the bidirectional TSCN is worth using. Details about the underlying performance trade-offs are discussed in Section 8.

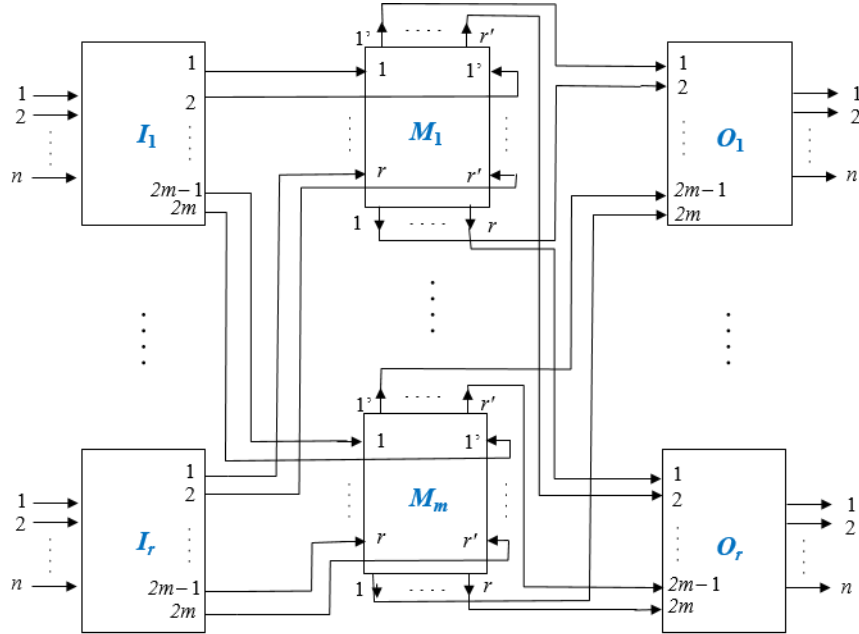


Figure 4. Bidirectional TSCN, denoted by $C_B(n, m, r)$, using modified XBSs in bidirectional mode in the middle stage.

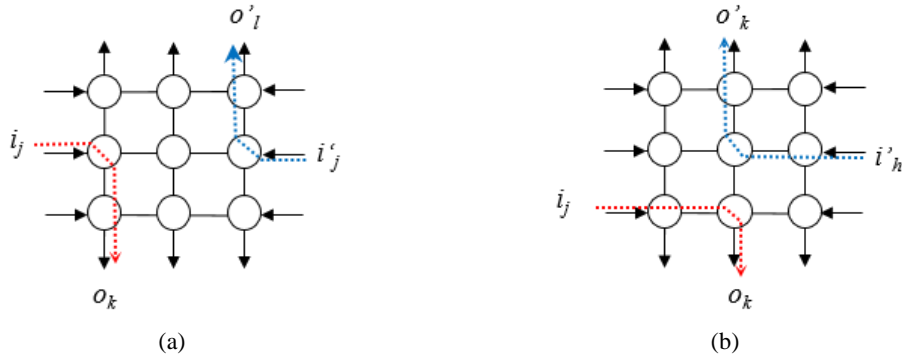


Figure 5. Sharing of a single row/column with a pair of routes in M_y in a disjoint manner. (a) A pair of routes may simultaneously coexist in a column when $l \geq k$; (b) A pair of routes may simultaneously coexist in a row when $h \leq j$

5. Rearrangeably non-blocking bidirectional TSCNs

5.1. Theoretical lower bound of m

In a conventional TSCN, such as the one shown in [Figure 1], n input ports in I_x correspond to output ports through m middle switches over a single link between stages. It is evident that the lower bound of m for non-blocking is $m = n$. In the bidirectional TSCN depicted in Fig. 4, there is a pair of links between every pair of switches. This duplicated link configuration allows two routes between a pair of XBSs, and m is reduced to $n/2$ for a special connection request; this is the case, for example, when $l = k$ and $j = h$ hold in [Figure 5a] and [Figure 5b], respectively. We refer to this special pattern as a set of compact connections. In general,

however, two connections require three row/column resources, as shown again in [Figure 5a] and [Figure 5b], although they require four row/column resources in conventional TSCNs. Consequently, our proposition for the lower limit of m for the bidirectional TSCN, denoted by m_L , is as follows:

$$m_L = \left\lceil \frac{3}{f_4} n \right\rceil, \quad (1)$$

where $\lceil * \rceil$ denotes a ceiling function.

Conventional TSCNs with minimum number of middle switches, i.e., $m = n$, become rearrangeably non-blocking. The number of rearrangements is given by $r - 1$ in a worst-case scenario in which rearrangements are confined within a pair of middle switches [25]. In the diminished bidirectional TSCN with $m_L < n$, every middle switch accommodates up to $4r/3$ connections. There is no definite boundary for a set of r connections, unlike conventional TSCs. In other words, the whole set of middle switches in the diminished bidirectional TSCN can be virtually seen as a single switch, similar to triangular switches, for which the number of rearrangements increases to $N - 1$. Consequently, the number of rearrangements for $CB(n, m_L, r)$ in a worst-case scenario, denoted by $RB(n, m_L, r)$, is expressed as follows:

$$R_B(n, m_L, r) = N - 1 \quad (2)$$

The elaborate mathematical proofs of Eqs. (1) and (2) are out of the scope of the study; however, we verified the validity of Eq. (1) through the simulations presented in Section 7.

5.2. Rearrangement for the case $m = n$

Although non-interruptive rearrangement techniques were developed [26], it is necessary to minimize the number of rearrangements to address high-speed switching applications. Here, we discuss how the number of rearrangements can be reduced for a typical bidirectional TSC with $m = n$, denoted as $R_B(n, n, r)$. In I_x of $C_B(n, n, r)$, we assume that an input signal i_j ($1 \leq j \leq n$) is forwarded to either o_k or o'_k ($1 \leq k \leq n$). This restriction on routing allows a simplified switch configuration of I_x , as shown in [Figure 6], where the j -th input signal is switched to either o_k or o'_k through an additional 1×2 switch. Note that the switch size of I_x becomes $n \times n$, instead of $n \times 2n$ as in Fig. 4, and there is at most a single signal on each row of I_x . It is evident that no blocking occurs in I_x because neither a row nor a column is shared by two signals there. In the middle stage, every row of M_y also has a single signal, similar to I_x , because it accepts a signal from either a left or right inlet. Therefore, no blocking can occur in a row of M_y . However, blocking can occur in a column of M_y as a result of two signals sharing that column. In M_y shown in Fig. 7a, the solid rectangular route between i_j and o_k denotes an existing connection, whereas the dashed route between i'_h and o'_k represents a new connection to be set up. Blocking occurs when these connections overlap in a column (i.e., $h > j$). However, note that i'_h and o'_k are idle because a new connection must be routed through idle ports. Note also that i'_j and i_h are idle as well because of the exclusive routing on a row in M_y . Under such conditions, the blocking will be resolved by diverting the existing connection to alternate routes through the same row, i.e., i'_j to o'_k , as shown in [Figure 7b]. Consequently, $C_B(n, n, r)$ requires a single rearrangement at most, regardless of n or r . Accordingly, $R_B(n, n, r)$ is expressed as follows:

$$R_B(n, n, r) = 1. \quad (3)$$

The simplicity of the rearrangement control described above means that the complexity of rearrangement is $O(1)$, whereas the complexity in the conventional $C(n, n, r)$ is $O(r)$.

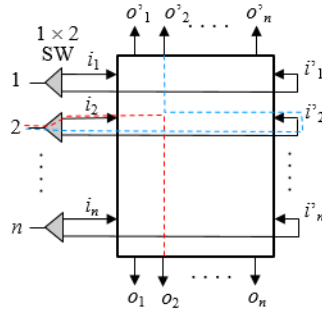


Figure 6. Design example of I_x for $C(n, n, r)$. Note that an input signal is routed to either o_k or o'_k ($1 \leq k \leq n$) through a 1×2 switch and the number of outlets is reduced to n instead of $2n$, although n additional 1×2 switches are required.

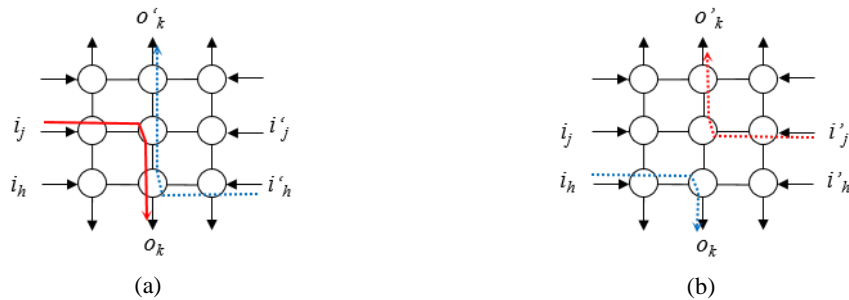


Figure 7. Blocking and unblocking at M_y . (a) Blocking state in a column; (b) Unblocking by diverting an existing connection (i_j, o_k) to (i'_j, o'_k) .

6. Wide-sense non-blocking bidirectional TSCNs

In the previous section, we found that row/column sharing reduces the lower bound of m for RNB bidirectional TSCNs. We further expect that both WSNB and SNB types can be realized by increasing m , similar to conventional TSCNs. Given that row/column sharing should be maintained to keep m as small as possible, bidirectional TSCs that require no rearrangements become WSNB. Here, we introduce a primitive type of WSNB bidirectional TSCN, shown in Fig. 8, based on a conventional SNB TSCN for which the minimum m is given by the following expression:

$$m_{SNB} = 2n - 1. \quad (4)$$

Eq. (4) holds in the worst-case scenario as follows. Assume that $n - 1$ input ports of an input switch I_i correspond to output switches, excluding O_k , through a set of $n - 1$ middle switches M_j^i ($j = 1, \dots, n - 1$), while $n - 1$ output ports of the output switch O_k correspond to input switches, excluding I_i , through a different set of $n - 1$ middle switches M_h^k ($h = 1, \dots, n - 1$). When a connection request occurs between the last idle input port of I_i and the last idle output port of O_k , an extra middle switch M_x is necessary for SNB TSCNs. The sum of middle switches in these three sectors is $2n - 1$. In bidirectional TSCNs, each independent set of $n - 1$ middle switches, as depicted in Fig. 8, can be reduced to m_L , as shown in Eq. (1). Consequently, the WSNB condition for bidirectional TSCNs is expressed as follows:

$$m_{WSNB} = 2 \left\lceil \frac{3}{4}(n-1) \right\rceil + 1 \leq \left\lceil \frac{3}{2}n \right\rceil + 1, \quad (5)$$

where the equality holds when $n = 4d$ ($d = 1, 2, 3, \dots$) Here, we see that m_{WSNB} is smaller than m_{SNB} by approximately 25%. The WSNB bidirectional TSCN requires a certain call packing algorithm for row/column sharing, the details of which are discussed below.

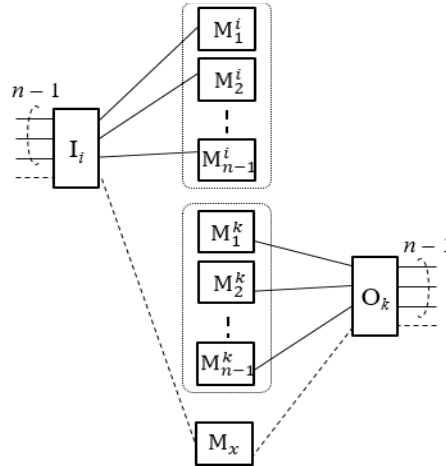


Figure 8. Worst-case scenario for WSNB bidirectional TSCs based on conventional SNB TSCs

7. Methodology and simulation results

The methodology employed in this study involves building simulation models of our proposed switch using C programming. We then examined the non-blocking performance of bidirectional TSCNs through simulation of call connection and disconnection. The number of middle stage switches which determine the non-blocking properties was observed in relation to blocking occurrence in the simulation. In the simulation, we focused on the middle switches in WSNB bidirectional TSCNs because no blocking occurs in the input and output switches. Two-dimensional data arrays were used to represent the connections at every inlet and outlet of the XBSs in the middle stage. The first dimension of such arrays represented the XBS number s , $1 \leq s \leq m$, whereas the second dimension represented the inlet or outlet number of the XBS l , $1 \leq l \leq r$. The content referred to by these two arguments indicated an associated inlet or outlet number t , $0 \leq t \leq r$. Note that $t = -1$ indicated an idle state i.e. no connection existing at that port. Fig. 9a shows a simplified flowchart of the simulation implementation. The simulation procedure begins with the initialization of all the data arrays to ensure that no initial connection exists in the bidirectional TSCNs. Next, an initial call setup is performed by assigning the inlet of the XBSs with the destination outlets and linking the outlets with the source inlets. We assume an initial call setup with 100% load.

We examined a number of initial call connection patterns and found that the set of compact connections defined in Section 5.1 is suitable for imposing the worst situation. Next, an arbitrary pair of connections is selected and disconnected. After the disconnection, the destinations are swapped, and an attempt to reconnect the two new requests is made. The algorithm begins by searching for an available route for the first request, and if it successfully finds the route, it sets it up and then searches for an available route for the second request in the same way.

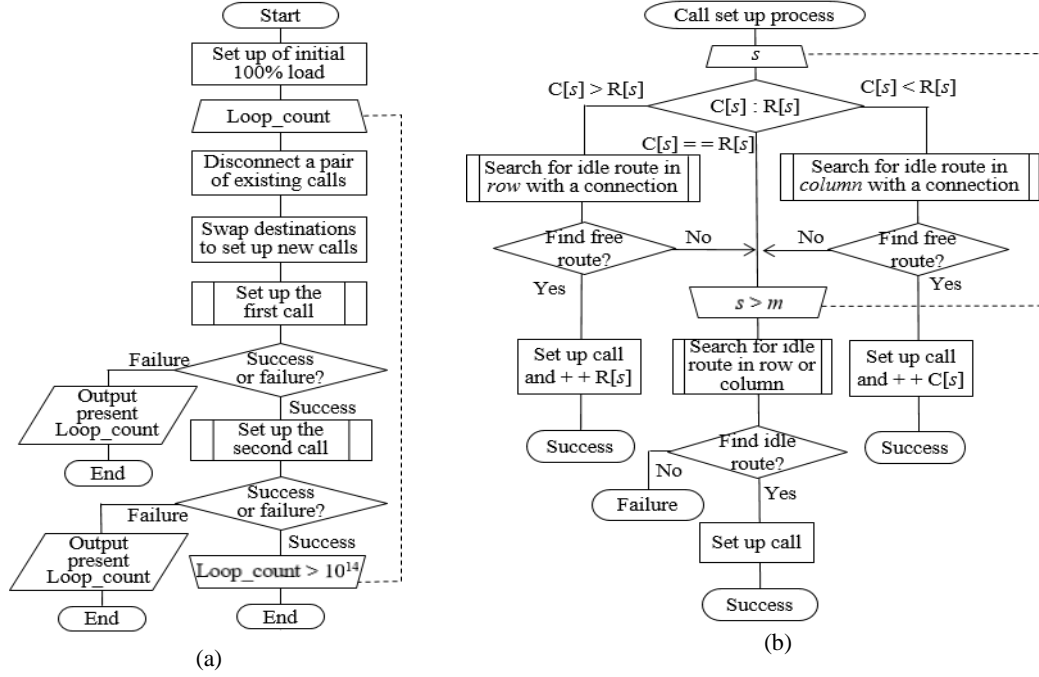


Figure 9. Algorithm flowchart to test the call setup in $CB(n, m, r)$. (a) Whole simulation process; (b) Details of path search for setting up the first and second calls

Note that during the route search, row/column pair connections are given priority, i.e., the algorithm always seeks to establish a row/column pair connection for a new call so as to use the switch resources efficiently. We define two parameters, $C[s]$ and $R[s]$, that represent the number of pairs formed in the column and row directions, respectively, in the s -th XBS. A detailed flowchart of the free-route search for the first and second calls is shown in Fig. 9b. An idle route is sought in the XBSs in sequence (or $s = 1$ to m). At the s -th middle switch, $C[s]$ and $R[s]$ are compared. If $C[s] > R[s]$, an idle route is sought in the row direction to achieve a load balance between $C[s]$ and $R[s]$. If $C[s] < R[s]$, an idle route is sought in the column direction to increase $C[s]$. If $C[s] = R[s]$, the algorithm skips from s to $s + 1$. If there are no row/column pairs to be made, then the call could be set up using a default route search, which does not necessarily search for pairs. If no available route is found, it is concluded that a call could not be set up, blocking occurred in the bidirectional TSCN for that particular request, and the procedure ends in failure. Note that a simple first-fit strategy is used for every path search. Although our path search algorithm requires several runs to search for an available route through each of the middle switches, the complexity for setting up a connection is $O(mr)$, which is the same as in conventional TSCNs with SNB capability.

In the simulation, $n = r$ was assumed, i.e., $N = n^2$, and m was varied for several pairs of fixed n and r to check the point at which blocking in the bidirectional TSCNs did not occur. The maximum number of loops was 1×10^{14} for each setting of n . We deemed that this was sufficient to test for non-blocking conditions because we observed that blocking in conventional TSCNs, i.e., $C(n, m, n)$, was always detected within a loop count of 1×10^{10} , as shown in [Figure 10a], where $n = 8, 12, \text{ and } 16$.

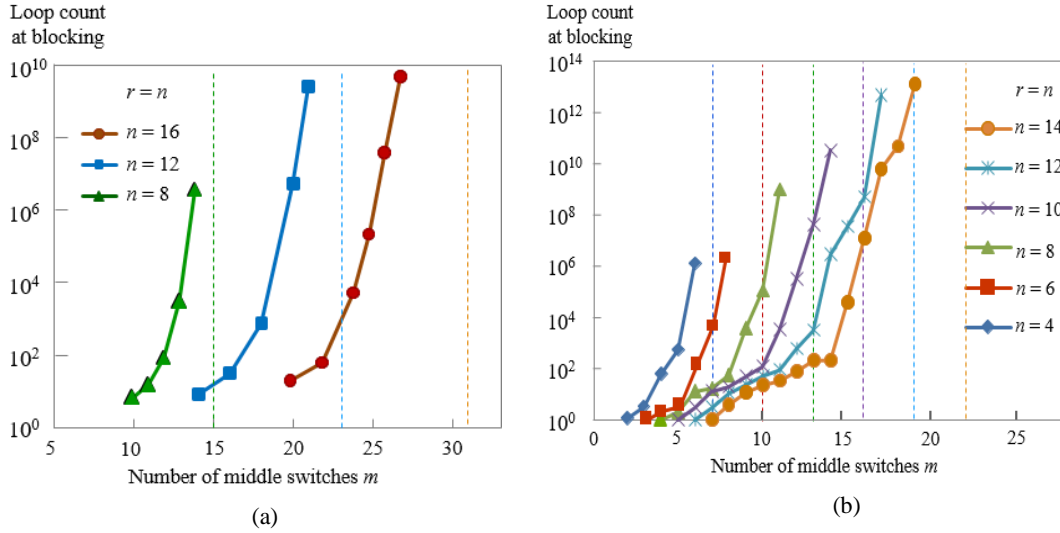


Figure 10. Loop count when the first blocking occurred vs. the number of middle switches (m).
 (a) For conventional TSCNs; (b) For bidirectional TSCNs

8. Discussion

As can be seen in [Figure10a], the values $m_{SNB} = 15, 23,$ and 31 , given by Eq. (4), are indicated as vertical dotted lines; in these cases, no blocking was observed. Fig. 10b shows the loop counts when the first blocking occurred in $C_B(n, m, n)$ as a function of m for $n = 4, 6, 8, 10, 12,$ and 14 . Each vertical dotted line corresponds to m_{WSNB} given by Eq. (5). The value of m increased until no blocking occurred for the maximum number of loops. Table 1 shows a relationship of n and N of the results from fig. 10b. It shows the number of middle stage switches at which blocking in the switch is occurring and the point at which blocking is no longer detected. Note that blocking continued to occur until the number of middle switches m was equal to or less than $\lceil 3n/2 \rceil$. Blocking ceased when the number of middle-stage switches reached $\lceil 3n/2 \rceil + 1$. Consequently, we found that Eq. (5) holds as a test of the WSNB condition, although we performed simulations within a limited range of n and m . Given that Eq. (5) was derived from Eq. (1), which corresponds to the row/column-sharing scheme, we also verified Eq. (1) indirectly.

The theoretical analysis involved a consideration of switch performance for conventional and bidirectional TSCNs as summarized in Table 2 as a function of m , the maximum number of rearrangements, the total number of crosspoints, and the differential number of crosspoints to $C(n, n, r)$. We calculated the number of crosspoints in an $n \times m$ XBS as nm . For example, the numbers of crosspoints in the first, second, and third stages in $C(n, n, r)$ are respectively given by $n^2r, r^2n,$ and n^2r . As a result, the total number of crosspoints in $C(n, n, r)$ is $2n^2r + r^2n$, which results in $N(2n + r)$, as shown in Table 2, because $N = nr$ holds. Note that n and r are correlated to each other for a given N . We approximated several values in [Table 1] to identify the differences in performance easily. For example, both $\lceil x \rceil$ and $x \pm 1$ are approximated as x . The approximated values are denoted by \cong .

Note that there is a clear performance trade-off relation between the number of rearrangements and the total number of crosspoints. For example, $C(n, n, r)$ has $r - 1$ rearrangements but presents a minimum number of Crosspoint, while $C_B(n, m_{WSN}, r)$ and $C(n, 2n - 1, r)$ require no rearrangements at the cost of a significant increase in crosspoints. Interestingly, $C_B(n, m_{WSN}, r)$ and $C(n, 2n - 1, r)$ achieve no rearrangements by increasing the

crosspoints in the first and third stages (i.e., ‘ $4n$ ’ and ‘ $3n$ ’ in the rightmost column of Table 2), while $C_B(n, m_{WSN}, r)$ has a smaller number of crosspoints in the second stage (i.e., ‘ $r/2$ ’ in the rightmost column of Table 2). Note that $C_B(n, n, r)$ requires a single rearrangement at the cost of a moderate increase in crosspoints. $C_B(n, m_L, r)$ has a maximum number of rearrangements, but it presents a lower number of total crosspoints than $C(n, n, r)$ if $n - r/4 < 0$, i.e., $r > 4n$. Similarly, the difference in total crosspoints between $C_B(n, m_{WSN}, r)$ and $C(n, 2n - 1, r)$ is given by $N(n - r/2)$. Thus, $C_B(n, m_{WSN}, r)$ has a lower number of total crosspoints than $C(n, 2n - 1, r)$ if $n - r/2 < 0$, i.e. $r > 2n$. Consequently, the use of $C_B(n, m_L, r)$ and $C_B(n, m_{WSN}, r)$ is expected in switch configurations in which the size of the middle switches is twice or quadruple larger than that of the input and output switches.

Table 1. Summary of switch sizes and number of middle stage switches when blocking was last detected and when blocking was not detected

n	Size of switch (N x N)	Value of m when last blocking is detected	Value of m when no blocking is detected
2	4 x 4	3	4
4	16 x 16	6	7
6	36 x 36	9	□□
8	64 x 64	12	□□□
10	100 x 100	15	□□□
12	144 x 144	18	□□□
14	196 x 196	21	□□□

Table 2. Summary of switch performances for conventional and bidirectional TSCs

Types of TSCs	Number of middle switches	Number of rearrangements	Total number of crosspoints	Differential number of crosspoints to $C(n, n, r)$
$C(n, n, r)$	n	$r - 1$	$N(2n + r)$	0
$CB(n, m_L, r)$	$\lceil 3n/4 \rceil$	$N - 1$	$\cong N(3n + 3r/4)$	$\cong N(n - r/4)$
$CB(n, n, r)$	n	1	$\cong N(3n + r)$	$\cong Nn$
$CB(n, m_{WSN}, r)$	$\cong \lceil 3n/2 \rceil + 1$	0	$\cong 2N(3n + 3r/4)$	$\cong N(4n + r/2)$
$C(n, 2n - 1, r)$	$2n - 1$	0	$\cong 2N(2n + r)$	$\cong N(3n + r)$

9. Conclusion

In this study, we considered TSCNs using conventional XBSs, each of which composed of 2×2 BSEs arranged in a square array. First, we pointed out that XBSs have a number of idle ports unused. The purpose of our study was to use these ports. We introduced modified XBSs with an extra set of interconnection ports to improve TSCN performance. We then proposed a new type of TSCN in which the modified XBSs operate as bidirectional switches and row/column sharing may be implemented in a simple manner. Second, we investigated the non-blocking performance of bidirectional TSCNs through theoretical analysis. We showed that the lower bound of m for rearrangeably non-blocking capability can be expressed as $m = \lceil 3n/4 \rceil$, which is smaller than that of original TSCNs by 25% owing to row/column sharing. We further showed that when $m = n$, the number of rearrangements is reduced to one at most, regardless of n and r , while ordinary TSCs require $r - 1$ rearrangement in the worst-case scenario. Finally, we developed WSNB bidirectional TSCNs based on conventional SNB TSCNs. We also showed that their WSNB condition can be expressed as $m = \lceil 3n/2 \rceil + 1$, which is smaller than $m = 2n - 1$ for conventional SNB TSCNs by approximately 25%. We also tested the validity of the WSNB condition through simulations; the results support our propositions. Through performance comparison, we found that bidirectional TSCNs can be used in TSCNs in which

the size of the middle switches is larger than that of the input and output switches. Although our theoretical analysis indicates the viability of the bidirectional TSCNs, experimental analysis as well as further detailed theoretical analysis will be necessary to realize these networks fully. It will constitute a research subject for future study.

References

- [1] W. Kabacinski, C. -T. Lea, and G. Xue, "Guest editorial - 50th anniversary of clos networks," *IEEE Communications Magazine*, vol.41, no.10, pp.26-27, (2003), DOI:10.1109/MCOM.2003.1235590
- [2] Q. Cheng, M. Bahadori, Y. Hung, Y. Huang, N. Abrams, and K. Bergman, "Scalable microring-based silicon Clos switch fabric with switch-and-select stages," *IEEE Journal of Selected Topics in Quantum Electronics*, vol.25, no.5, pp.1-11, (2019), Art no. 3600111, DOI:10.1109/JSTQE.2019.2911421
- [3] L. Wang, T. Ye, and T. T. Lee, "A parallel route assignment algorithm for fault-tolerant Clos networks in OTN switches," *IEEE Transactions on Parallel and Distributed Systems*, vol.30, no.5, pp.977-989, (2019), DOI:10.1109/TPDS.2018.2880782
- [4] O. T. Sule and R. Rojas-Cessa, "TRIDENT: A load-balancing clos-network packet switch with queues between input and central stages and in-order forwarding," *IEEE Transactions on Communications*, vol.67, no.10, pp.6885-6896, (2019), DOI:10.1109/TCOMM.2019.2926730
- [5] D. M. Marom et al, "Survey of photonic switching architectures and technologies in support of spatially and spectrally flexible optical networking," *IEEE/OSA Journal of Optical Communications and Networking*, vol.9, no.1, pp.1-26, (2017), DOI: 10.1364/JOCN.9.000001
- [6] G. I. Papadimitriou, C. Papazoglou, and A. S. Pomportsis, "Optical switching: Switch fabrics, techniques, and architectures," *Journal of Lightwave Technology*, vol.21, no.2, pp.384-405, (2003), DOI:10.1109/JLT.2003.808766
- [7] H. Obara, "Reduced crossbar switch with minimum number of switching cells," *Electronics Letters*, vol.44, no.14, pp.888-889, (2008), DOI:10.1049/el:20083528
- [8] H. Obara, "Design of optical multi/demultiplexers composed of bidirectional 2x2 switch elements for reducing component count," *Electronics Letters*, vol.51, no.15, pp.1182-1184, (2015), DOI:10.1049/el.2015.1526
- [9] C. -T. Lea, "Expanding the switching capabilities of optical cross connects," *IEEE Transactions on Communications*, vol.53, no.11, pp.1940-1944, (2005), DOI:10.1109/TCOMM.2005.858662
- [10] H. Obara, "Cascaded versus parallel architectures of two-stage optical crossbar switches with an extra set of inputs and outputs," *IET Optoelectronics*, vol.12, no.4, pp.196-201, (2018), DOI:10.1049/iet-opt.2017.0096
- [11] S. Ohta, "The number of rearrangements for Clos networks-new results," *Theoretical Computer Science*, vol.814, pp.106-119, (2020), DOI:10.1016/j.tcs.2020.01.2018
- [12] C. Clos, "A study of nonblocking switching networks," *Bell Syst. Tech. J.*, vol.32, pp.406-424, (1953), DOI:10.1002/j.1538-7305.1953.tb01433.x
- [13] M. C. Paul, "Re switching of connection networks," *Bell Syst. Tech. J.*, vol.41, pp.833-855, (1962), DOI:10.1002/j.1538-7305.1962.tb00478.x
- [14] F. H. Chang, J. Y. Guo, F. K. Hwang, and C. K. Lin, "Wide-sense nonblocking for symmetric or asymmetric 3-stage clos networks under various routing strategies," *Theoretical. Computer Science*, vol.314, no.3, pp.375-386, (2004), DOI:10.1016/j.tcs.2003.12.021
- [15] A. Jajszczyk and G. Jekel, "A new concept-repackable networks," *IEEE Transactions on Communications*, vol.41, no.8, pp.1232-1237, Aug. (1993), DOI:10.1109/26.231967
- [16] H. Obara "Strictly non-blocking three-quarter crossbar switch with simple switch control," *IET Electronics Letters*, vol.52, no.25, pp.2051-2053, (2016), DOI:10.1049/el.2016.3561
- [17] K. Goossens, L. Mhamdi, and I. V. Senin, "Internet-router buffered crossbars based on networks on chip," *12th Euromicro Conference on Digital System Design, Architectures, Methods and Tools, Patras, Greece*, pp.365-374, (2009), DOI:10.1109/DSD.2009.211

- [18] L. Mhamdi, K. Goossens, and I. V. Senin, "Buffered crossbar fabrics based on networks on chip," 8th Annual Communication Networks and Services Research Conference, Montreal, QC, pp.74-79, (2010), DOI:10.1109/CNSR.2010.18
- [19] F. Hassen and L. Mhamdi, "Congestion-aware multistage packet-switch architecture for data center networks," IEEE Global Communications Conference (GLOBECOM), Washington DC, pp.1-7, (2016) DOI:10.1109/GLOCOM.2016.7841681
- [20] F. Hassen and L. Mhamdi, "High-capacity clos-network switch for data center networks," IEEE International Conference on Communications (ICC), Paris, pp.1-7, (2017), DOI:10.1109/ICC.2017.7997147
- [21] T. S. El-Bawab, "Optical switching," 1st ed., Springer, Berlin, DE, **(2010)**
- [22] K. Tanizawa, K. Suzuki, K. Ikeda, S. Namiki, and H. Kawashima, "Novel PILOSS port assignment for compact polarization-diversity Si-wire optical switch," Optical Fiber Communications Conference and Exhibition (OFC), Anaheim, CA, paper number M31-6, **(2016)**
- [23] F. K. Hwang, "The mathematical theory of nonblocking switching networks," 2nd ed., World Scientific, London, UK, pp.59-67, **(2004)**
- [24] S. Ohta, "A new result on rearrangeable 3-stage Clos networks," 28th International Telecommunication Networks and Applications Conference (ITNAC), Sydney, NSW, pp.1-6, **(2018)**, DOI:10.1109/ATNAC.2018.8615439
- [25] W. Kabacinski, "Nonblocking electronic and photonic switching fabrics," 1st ed., Springer, Berlin, DE, pp.55-61, **(2005)**
- [26] F. K. Hwang, W. Lin, and V. Lioubimov, "On non-interruptive rearrangeable networks," IEEE/ACM Transactions on Networking, vol.14, no.5, pp.1141-1149, **(2006)**, DOI:10.1109/TNET.2006.882846